ARTICLE
Journal of Cellular Biochemistry 105:801–813 (2008)

Journal of Cellular Biochemistry

Regulatory Expression of *Brachyury* and *Goosecoid* in P19 Embryonal Carcinoma Cells

Kohei Nakaya,[1] Masaru Murakami,[1] and Masayuki Funaba[2*]

[1]*Laboratory of Molecular Biology, Azabu University School of Veterinary Medicine, Sagamihara 229-8501, Japan*

[2]*Laboratory of Nutrition, Azabu University School of Veterinary Medicine, Sagamihara 229-8501, Japan*

ABSTRACT

Mouse P19 embryonal carcinoma cells can differentiate into various cell types depending on culture conditions. Here we show that the expression of the mesodermal genes *Brachyury* (*Bra*) and *Goosecoid* (*Gsc*) are under regulatory control in P19 cells. When P19 cells were cultured in a tissue culture dish in the presence of serum, *Bra* and *Gsc* were unexpectedly expressed. Expression of *Bra* and *Gsc* was greatly reduced with culture time, and expression levels at 144 h of culture were below 25% those at 48 h of culture. Members of the Tgf-β family such as Activin and Nodal have been known to up-regulate expression of mesodermal genes. Treatment with SB431542, an Alk4/5/7 inhibitor, decreased *Bra* and *Gsc* in a dose-dependent manner, whereas it induced the expression of the neuroectodermal genes *Mash-1* and *Pax-6*. Quantitative RT-PCR and dsRNAi transfection indicated *Nodal* as a possible ligand responsible for the regulation of *Bra* and *Gsc*. In addition, exogenous Nodal increased expression of *Bra* and *Gsc* in a dose-dependent manner. Serum concentration in culture medium positively related to expression of *Nodal*, *Bra*, *Gsc*, and *Cripto*, which encodes a membrane-tethered protein required for Nodal signaling. Addition of the culture supernatant of P19 cells at 144 h of culture to medium decreased expression of these genes. The present study reveals that stimulation and inhibition of the Nodal pathway increases mesodermal genes and neuroectodermal genes, respectively, indicating the importance of control of *Nodal* and *Cripto* expression for mesodermal formation and neurogenesis. J. Cell. Biochem. 105: 801–813, 2008.

KEY WORDS: P19; MESODERMAL GENE; GENE EXPRESSION; NODAL; CRIPTO

Embryonic stem (ES) cells are pluripotent cells derived from the inner cell mass of blastocysts. ES cells can proliferate while maintaining pluripotency, and they can also differentiate into a large number of somatic cell types during early development. Many studies focus on factors affecting mouse ES cell pluripotency and differentiation into a specific cell type, but a comprehensive understanding of the mechanisms underlying self-renewal and differentiation of ES cells is not yet fully understood [Niwa, 2001; Burdon et al., 2002; O'Shea, 2004].

Mouse P19 embryonal carcinoma cells resemble the inner cell mass of the early embryo, and have been used as a model system for studying early embryonic development and differentiation [McBurney, 1993]. P19 cells can differentiate into cells that are endoderm-like, neuroectoderm-like or muscle-like, depending on culture conditions [McBurney, 1993]. Treatment of aggregated P19 cells in a bacterial grade culture dish with 0.5–1.0% DMSO followed by plating onto a tissue culture grade dish leads to differentiation toward muscle-like cells, whereas the treatment of aggregated P19 cells with low (10 nM) and high (1 μM) concentrations of retinoic acid (RA) during culture in a bacterial grade culture dish results in differentiation into endoderm-like and neuroectoderm-like cells, respectively [Jones-Villeneuve et al., 1982; McBurney et al., 1982; McBurney, 1993].

Brachyury (Bra), a member of the T-box transcription factors, mainly functions in the early specification of posterior mesoderm and formation of the notochord [Technau, 2001]. Goosecoid (Gsc), a paired-like homeobox gene expressed in the vertebrate organizer, functions as a dorsoventral patterning of mesoderm at the early gastrula stage [Boncinelli and Mallamaci, 1995]. Both are early mesodermal genes, and are up-regulated by treatment with Activin, a member of the Tgf-β family, in Xenopus animal caps [Smith et al., 1990; Cho et al., 1991].

When analyzing the regulation of P19 cell differentiation, we noticed that the mesodermal genes *Bra* and *Gsc* were expressed in

Grant sponsor: Japan Society for the Promotion of Science; Grant numbers: 17580262, 15580268, 18580299; Grant sponsor: Foundation for Japanese Private School Promotion.

Dr. Masayuki Funaba's present address is Laboratory of Nutritional Science, Kyoto University Graduate School of Agriculture, Kyoto 606-8502, Japan.

*Correspondence to: Dr. Masayuki Funaba, Laboratory of Nutritional Science, Kyoto University Graduate School of Agriculture, Kyoto 606-8502, Japan. E-mail: mfunaba@kais.kyoto-u.ac.jp

Received 9 January 2008; Accepted 8 July 2008 • DOI 10.1002/jcb.21883 • 2008 Wiley-Liss, Inc.

Published online 26 August 2008 in Wiley InterScience (www.interscience.wiley.com).

monolayer P19 cells cultured in a tissue culture grade dish in the presence of serum. This was unexpected, since previous studies indicate that P19 cells do not express *Bra* and *Gsc* without induction of differentiation [Pruitt, 1994; Pratt et al., 1998]. Thus, the present study explored factors affecting expression of *Bra* and *Gsc* in monolayer P19 cells.

MATERIALS AND METHODS

MATERIALS

SB431542, an Alk4/5/7 inhibitor [Callahan et al., 2002; Inman et al., 2002], was purchased from TOCRIS. PD98059 and SB203580 were purchased from Calbiochem. SP600125 was purchased from BIOMOL Research Laboratories (Plymouth Meeting, PA). Recombinant mouse Nodal was purchased from R & D Systems. Rabbit polyclonal antibody against phospho-Smad2 (Ser465/Ser467) was purchased from Cell Signaling Technology. Mouse monoclonal antibody against β-actin (AC-15) was purchased from Abcam (Cambridge, UK). Goat polyclonal antibody against Lefty (M-20) was obtained from Santa Cruz Biotechnology and Blue Sepharose 6 Fast Flow beads from GE Healthcare.

CELL CULTURE

P19 cells, which were provided by the Institute of Development, Aging and Cancer, Tohoku University, were cultured in αMEM with 6% FCS, 2 mM L-glutamine, 100 U/ml penicillin and 100 μg/ml streptomycin. Flow cytometric analyses indicated that P19 cells used in this study were diploid (data not shown). Establishment of a single cell clone from P19 cells was conducted using a cloning ring (Iwaki, Tokyo, Japan) or by limited dilution.

RNA ISOLATION AND RT-PCR

Total RNA from P19 cells was isolated using an RNA isolation kit (RNeasy, Qiagen), followed by treatment with DNase I (Invitrogen) to digest genomic DNA and subsequent cDNA synthesis using a cDNA synthesis kit (SuperScript III First-Strand Synthesis System, Invitrogen). For experiments in monolayer P19 cells, RNA was recovered from the attached cells. PCR was carried out with cDNA synthesized from 5 ng of total RNA in order to detect pluripotent differentiation markers (*Nanog* and *Oct-3/4*) [Okamoto et al., 1990; Chambers et al., 2003; Mitsui et al., 2003], neuroectodermal markers (*Mash-1* and *Pax-6*) [Johnson et al., 1990; Walther and Gruss, 1991], mesodermal markers (*Bra* and *Gsc*) [Rashbass et al., 1991; Blum et al., 1992], components of the Tgf-β family, and a housekeeping gene (*G3pdh*). After 5 min at 95°C, the reaction was subject to a cycle profile of 30 s at 95°C, 30 s at annealing temperature, and 45 s at 72°C, followed by 5 min at 72°C. For detection of *Smad6*, denaturation was conducted at 98°C. The annealing temperature for detection of pluripotent differentiation markers, neuroectodermal markers, and mesodermal markers was 54°C, and for the remaining genes it was 58°C. The products were separated on a 1.5% agarose gel and stained with ethidium bromide, followed by visualization under ultraviolet light. The PCR primers and number of PCR cycles to detect pluripotent differentiation markers, neuroectodermal markers, mesodermal markers and the housekeeping gene are shown in Table I. The PCR primers and number of PCR cycles for detection of Tgf-β family gene transcripts are shown in Table II. The PCR primers for genes other than *Mash-1*, *Bra*, *Inhα*, *InhβA*, *InhβB*, and *Bmp-2* were set at the different exon, and no significant band was detected at the size of PCR product originated from genomic DNA (data not shown). RT-PCR analyses to examine gene expression were conducted at least two times.

QUANTITATIVE REAL-TIME RT-PCR

Quantitative real-time RT-PCR was performed as described previously [Funaba et al., 2003]. The PCR primers for *G3pdh* were as described [Funaba et al., 2003]. The PCR primers for real-time RT-PCR to examine transcript levels of *Bra*, *Gsc*, *Nodal*, *Cripto*, *Gdf-1*, *Gdf-11*, *Mash-1* and *Pax-6* were as follows: nt 906–928 and 978–960 for *Bra*, 695–716 and 769–756 for *Gsc*, 730–750 and 805–786 for *Nodal*, 201–221 and 277–256 for *Cripto*, 356–377 and 450–429 for *Gdf-1*, 710–731 and 787–768 for *Gdf-11*, 708–726 and 777–757 for *Mash-1*, and 427–446 and 498–478 for *Pax-6*. The levels of gene expression in each sample were determined using the relative

TABLE I. Oligonucleotide PCR Primers to Detect Pluripotent Differentiation Markers, Neuroectodermal Markers, Mesodermal Markers and Housekeeping Gene by RT-PCR Analyses and PCR Cycles

	Oligonucleotide (nt)[a]		Size (bp)		GeneBank
	5′-primer	3′-primer	PCR product	PCR cycles	accession number
Pluripotent differentiation					
Nanog	−190 to −167	297–279	487	30	AF507043
Oct-3/4	493–516	805–786	313	35	NM_013633
Neuroectodermal marker					
Mash-1	255–276	555–534	301	30	NM_008553
Pax-6	322–341	499–478	178	30	NM_013627
Mesodermal marker					
Bra	−60 to −38	206–184	266	30	NM_009309
Gsc	401–423	775–754	375	30	NM_010351
Housekeepking gene					
G3pdh	273–292	1,001–982	729	27	BC083065

[a]The nt + 1 is defined as the start site of the coding region.

TABLE II. Oligonucleotide PCR Primers to Detect Molecules Related to Signaling of the Tgf-β Family by RT-PCR Analyses and PCR Cycles

	Oligonucleotide (nt)[a]		Size (bp)		GeneBank accession number
	5′-primer	3′-primer	PCR product	PCR cycles	
Ligand					
Tgf-β1	462–482	1,013–994	552	35	NM_011577
Tgf-β2	521–543	1,204–1,184	684	35	NM_009367
Tgf-β3	635–654	1,074–1,055	440	35	NM_009368
Inhα	341–360	884–865	544	35	NM_010564
InhβA	598–617	1,202–1,183	605	35	NM_008380
InhβB	66–83	346–331	281	35	NM_008381
Nodal	19–38	662–643	644	30	NM_013611
Bmp-2	363–382	909–890	547	35	NM_080708
Bmp-4	206–227	965–945	760	35	NM_007554
Bmp-7	465–484	1,251–1,232	787	35	NM_007557
Gdf-1	356–377	450–429	783	30	NM_008107
Gdf-8	338–357	757–738	420	35	NM_010834
Gdf-11	183–203	559–540	377	30	AF092734
Lefty-1	725–744	1,061–1,042	271	35	NM_010094
Lefty-2	283–303	861–841	228	35	NM_177099
Modulator					
Follistatin	256–275	897–878	642	30	Z29532
Flrg	141–160	640–621	500	35	NM_031380
Cripto	103–122	405–386	303	30	NM_011562
Cryptic	116–135	469–450	354	35	NM_007685
Cerberus1	388–390	1,078–1,059	691	35	NM_009887
Cerberus2	3–21	399–380	397	35	NM_201227
Type I receptor					
Alk1	855–874	1,173–1,154	319	35	NM_009612
Alk2	875–894	1,419–1,400	545	35	NM_007394
Alk3	408–427	988–969	581	35	NM_009758
Alk4	884–903	1,513–1,494	630	35	NM_007395
Alk5	488–507	1,311–1,290	824	35	NM_009370
Alk6	882–901	1,371–1,353	490	35	NM_007560
Alk7	431–452	1,005–984	575	35	NM_001033369
Type II receptor					
TβRII	258–277	817–798	560	35	NM_009371
ActRII	835–854	1,537–1,518	703	35	NM_007396
ActRIIB	479–498	1,407–1,389	929	35	NM_007397
BmpRII	2,222–2,241	3,035–3,016	814	35	NM_007561
Signal mediator					
Smad1	306–325	924–905	619	35	NM_008539
Smad2	551–570	1,396–1,377	846	35	NM_010754
Smad3	642–661	1,277–1,254	636	35	NM_016769
Smad4	645–664	1,447–1,428	803	35	NM_008540
Smad5	754–773	1,390–1,371	637	35	NM_008541
Smad6	516–535	917–898	402	35	NM_008542
Smad7	532–554	1,187–1,167	656	35	NM_008543
Smad8	516–535	945–924	430	35	NM_019483

[a]The nt + 1 is defined as the start site of the coding region.

standard-curve method. The relative amount of cDNA of *Bra*, *Gsc*, *Nodal*, *Cripto*, *Gdf-1*, *Gdf-11*, *Mash-1* and *Pax-6* was expressed as a ratio with *G3pdh* cDNA. The expression levels of the genes at 48 h of culture of P19 cells treated with vehicle or control treatment was given a value of 100.

WESTERN BLOT

To examine phosphorylation of Smad2 at C-terminal serines, P19 cells were lysed in lysis buffer (20 mM Tris–HCl, pH 7.4, 150 mM NaCl, 1% Triton X-100, 1 mM PMSF, 1% aprotinin). After 10 min on ice, cell debris was removed by centrifugation at 15,000*g* for 2 min at 4°C. Protein (7 μg) in the supernatant was run on a 10% SDS–polyacrylamide gel, and transferred to PVDF membranes. After blocking the membranes (Ez Block, Atto, Tokyo, Japan), they were reacted with anti-phospho-Smad2 antibody, followed by reaction with peroxidase-conjugated anti-rabbit IgG antibody. Reacted proteins were visualized with a commercial kit (ECL Plus, Amersham Pharmacia Biotech). The membranes were then reacted with anti-β-actin antibody after stripping bound antibodies to monitor equal loading of cell lysates. We tried to examine total Smad2 expression, but failed to detect properly because of the sensitivity of the antibody.

To examine Lefty in the culture supernatant, culture medium was centrifuged at 15,000*g* for 5 min at 4°C. The supernatant (800 μl) was incubated with Blue Sepharose 6 Fast Flow beads (300 μl) for 1 h at 4°C. The unbound proteins were recovered by centrifugation at 950*g* for 5 min at 4°C, followed by concentration using the sodium deoxycholate-TCA method [Bensadoun and Weinstein, 1976]. Bound proteins were recovered by addition of 6× SDS–PAGE sample buffer. According to the manufacturer's data sheet, the

anti-Lefty antibody recognizes Lefty molecules migrating at 25 kDa, which were electrophoresed under reducing conditions, although the molecular species at 32 kDa in addition to the molecule at 25 kDa are also known [Meno et al., 1996]. Thus, SDS–PAGE was conducted under reducing conditions, and the band at 25 kDa was the focus of the present study.

RNA INTERFERENCE

dsRNAi to target expression of *Nodal* was synthesized by Samchully Pharmaceuticals (Seoul, Korea). The coding sequences were as follows: 5′-GAACUGGACUUUCACGUUUTT-3′. P19 cells were seeded at a density of 5×10^4 cells in 24-well plates and cultured overnight. dsRNAi of 20 pmol was transfected by use of Lipofectamine2000 according to manufacturer's protocol. At 24 h of transfection, cells were harvested and gene expression was examined by quantitative real-time RT-PCR.

DETERMINATION OF DOUBLING TIME

To determine doubling time of P19 cells, cells were plated in duplicate in 96-well plates at 670 Trypan blue-excluding viable cells/100 μl in αMEM with 6% FCS, 100 U/ml penicillin and 100 μg/ml streptomycin. Cell growth was determined by use of the CellTiter-Blue Cell Viability Assay Kit (Promega) at 24, 36, 48, 60, 72, and 84 h after plating. CellTiter-Blue reagent (20 μl) containing resazurin was added to the culture medium 2 h prior to measurement. Plates were analyzed in an ELISA plate reader at 570 nm with a reference wavelength of 600 nm. Data were plotted against time in a semi-logarithmic graph, and doubling time, the inverse of the slope of the graph, was calculated.

STATISTICAL ANALYSIS

Data were presented as the mean ± SE. Comparisons between groups were conducted using the Student's *t*-test. Results were considered statistically significant at $P < 0.05$.

RESULTS

UNDIFFERENTIATED P19 CELLS EXPRESS *Bra* AND *Gsc*

Previous studies have shown that when P19 cells are aggregated and exposed to DMSO or retinoic acid (RA), they differentiate into a variety of mesoderm-, endoderm- and ectoderm-like cells depending on the reagent and concentration [McBurney, 1993]. As a control study for analysis of factors controlling P19 cell differentiation, we examined the effects of cell aggregation and RA (1 μM) on gene expression of the pluripotent differentiation markers *Nanog* and *Oct-3/4*, the neuroectodermal markers *Mash-1* and *Pax-6*, and the mesodermal markers *Bra* and *Gsc* (Fig. 1A). Significant expression of *Nanog* and *Oct-3/4* was detected in untreated P19 cells, and treatment with aggregation or RA led to a decrease in gene expression of them, which is consistent with the notion that P19 cells are ES-like cells under unstimulated conditions. Consistent with previous studies [Johnson et al., 1992; Boudjelal et al., 1997; Pachernik et al., 2005], treatment with RA (1 μM) plus aggregation of P19 cells also induced expression of *Mash-1* and *Pax-6*. In addition, induction of *Mash-1* and *Pax-6* was also detected even in RA-treated monolayer P19 cells. Previous studies showed that monolayer-grown P19 cells induced expression of *Mash-1* and *Pax-6* in response to RA [Boudjelal et al., 1997; Pachernik et al., 2005], although the cells neither expressed neuron-specific *III β-tubulin* and *N-Cam* nor exhibited neuron-like cell morphology [Pachernik et al., 2005]. We also observed that aggregated P19 cells treated with RA but not

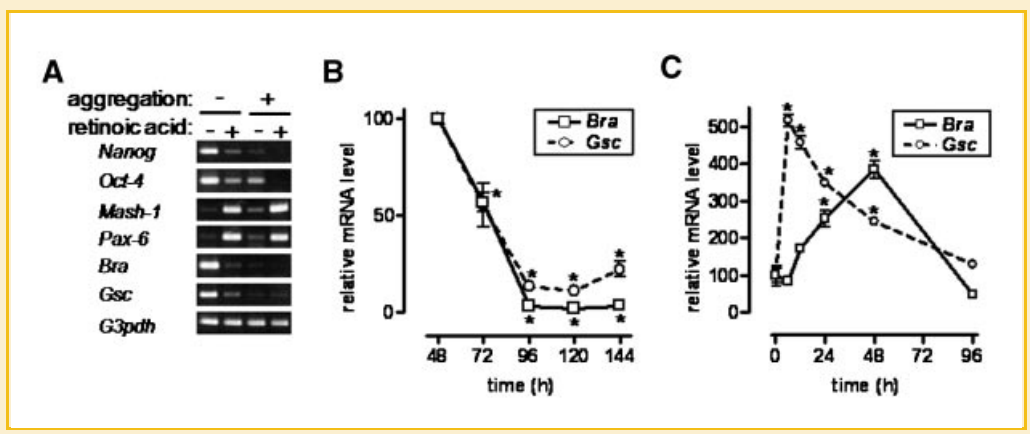

Fig. 1. *Bra* and *Gsc* are expressed in unstimulated P19 cells, and expression is decreased with time of culture. A: 3×10^4 and 15×10^4 cells were plated into tissue culture grade 35-mm dishes (aggregation: −) and bacterial culture grade 35-mm dishes (aggregation: +) in the presence (retinoic acid: +) or absence (retinoic acid: −) of RA (1 μM), respectively. At 3 days after culture, 8×10^3 cells obtained from a tissue culture grade 35-mm dish, and half of the cells recovered from a bacterial culture grade 35-mm dish were plated into 24-well tissue culture grade dishes in the absence of RA for an additional 3 days, respectively. RT-PCR was performed to detect pluripotent differentiation markers (*Nanog* and *Oct-3/4*), neuroectodermal markers (*Mash-1* and *Pax-6*), mesodermal markers (*Bra* and *Gsc*), and the housekeeping marker *G3pdh*. B,C: 8×10^3 cells were plated into tissue culture grade 24-well dishes. At the indicated times, attached cells were recovered, and quantitative real-time RT-PCR was performed to measure transcripts of *Bra* and *Gsc*. Gene expression was normalized to the transcript level of *G3pdh*, and the value at 48 h (B) or 0 h (C) of culture was set to 100. $^*P < 0.05$ as compared with the value at 48 h (B) or 0 h (C).

RA-treated monolayer P19 cells showed a round shape with neurite-like protrusions (data not shown).

Expression of mesodermal markers *Bra* and *Gsc* was clearly detected in untreated P19 cells (Fig. 1A). In view of the previous results [Pruitt, 1994; Pratt et al., 1998], this was unexpected. Expression disappeared in response to either aggregation treatment or RA treatment. To examine expression in detail, P19 cells were plated at 8×10^3 cells/well in a 24-well dish, and *Bra* and *Gsc* levels were examined by quantitative real-time RT-PCR (Fig. 1B). To know time-course changes in *Bra* and *Gsc* expression, culture medium was not changed throughout the study. Both genes were down-regulated with time of culture up until 96 h, and the decreased gene expression continued for an additional 48 h. Replating of P19 cells harvested at 144 h resulted in re-induction of *Bra* and *Gsc*, indicating reversible expression of *Bra* and *Gsc* (data not shown). In addition, expression of the pluripotent differentiation genes *Nanog* and *Oct-3/4* was detected at all times in the culture of monolayer P19 cells without RA treatment (data not shown). When gene expression during the earlier phase of culture was examined, changes in *Bra* expression with time of culture were different from those in *Gsc* expression; *Bra* expression gradually increases up to 48 h of culture, whereas *Gsc* expression reached a peak at 6 h of culture (Fig. 1C). P19 cells rapidly grew with a doubling time of ~13 h (Figs. 2 and 7B). Attached cells proliferated without changing morphology to reach confluency (~72 h), followed by the detachment of cells from the culture dish. The attached cells were trypan blue-exclusive throughout the culture (data not shown).

THE NODAL-CRIPTO PATHWAY POSITIVELY REGULATE *Bra* AND *Gsc* EXPRESSION IN P19 CELLS

Previous studies have shown that expression of *Bra* and *Gsc* is induced by Activin (homo- or heterodimer of Inhibin β (Inhβ) subunit) and Nodal, members of the Tgf-β family [Smith et al., 1990; Cho et al., 1991; Jones et al., 1996; Dyson and Gurdon, 1998]. As with other Tgf-β family members, Activin and Nodal signal via membrane-bound heteromeric serine kinase receptor complexes. In addition, expression of Cripto/Cryptic, a membrane-tethered protein, is necessary for Nodal signaling [Whitman, 2001]. Upon ligand binding to the type II receptor ActRII or ActRIIB, the receptor recruits, phosphorylates and activates the type I receptor (Alk4 for Activin and Alk4/7 for Nodal). Activated type I receptor serine/threonine kinases phosphorylate serine residues at or near the C-terminus of Smad2/3, and phospho-Smad2/3 form complexes with Smad4. The Smad complexes translocate into the nucleus, and regulate expression of target genes [Derynck and Zhang, 2003; Massagué et al., 2005]. The ligand-induced phosphorylation of Smad2/3 is the key event in this process, and thus we next examined changes in phosphorylation of Smad2 with time of culture to evaluate possible involvement of the Activin/Nodal pathway.

Western blotting revealed that phosphorylation of Smad2 tended to decrease with time of culture, although phospho-Smad2 did not disappear (Fig. 3A). In addition, treatment with SB431542, an inhibitor of Alk4/5/7 [Callahan et al., 2002; Inman et al., 2002], resulted in a dose-dependent decrease in *Bra* and *Gsc* (Fig. 3B,C). Decrease in *Bra* and *Gsc* was specific to SB431542 treatment; treatment with inhibitors for the MAP kinase pathways such as PD98059 (a MEK1 inhibitor), SB203580 (a p38 MAP kinase inhibitor), and SP600125 (a JNK inhibitor), did not remarkably decrease the levels of *Bra* and *Gsc*, although *Bra* and *Gsc* were slightly but significantly decreased by treatment with SB203580 (Fig. 3D,E). These results suggest that down-regulation of *Bra* and *Gsc* is mediated by attenuation of Tgf-β family signaling. To explore the ligand responsible for the down-regulation of *Bra* and *Gsc*, gene expression of molecules involved in Tgf-β family signaling was examined by RT-PCR analyses (Fig. 4). Expression of *Nodal* and *Cripto* but not *Cryptic*, *InhβA* and *InhβB* were detected at significant levels in P19 cells, suggesting that Nodal-Cripto but not Activin is a candidate ligand responsible for *Bra* and *Gsc* expression in

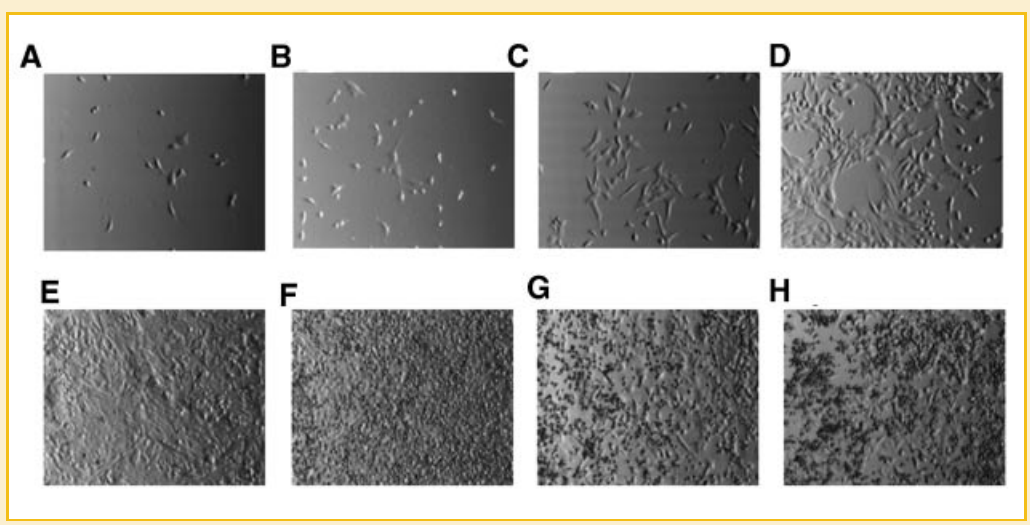

Fig. 2. Morphology of P19 cells during the culture. 8×10^3 cells were plated into tissue culture grade 24-well dishes. At 6 h (A), 12 h (B), 24 h (C), 48 h (D), 72 h (E), 96 h (F), 120 h (G), and 144 h (H) of the culture, attached cells were observed by phase contrast microscopy (100×).

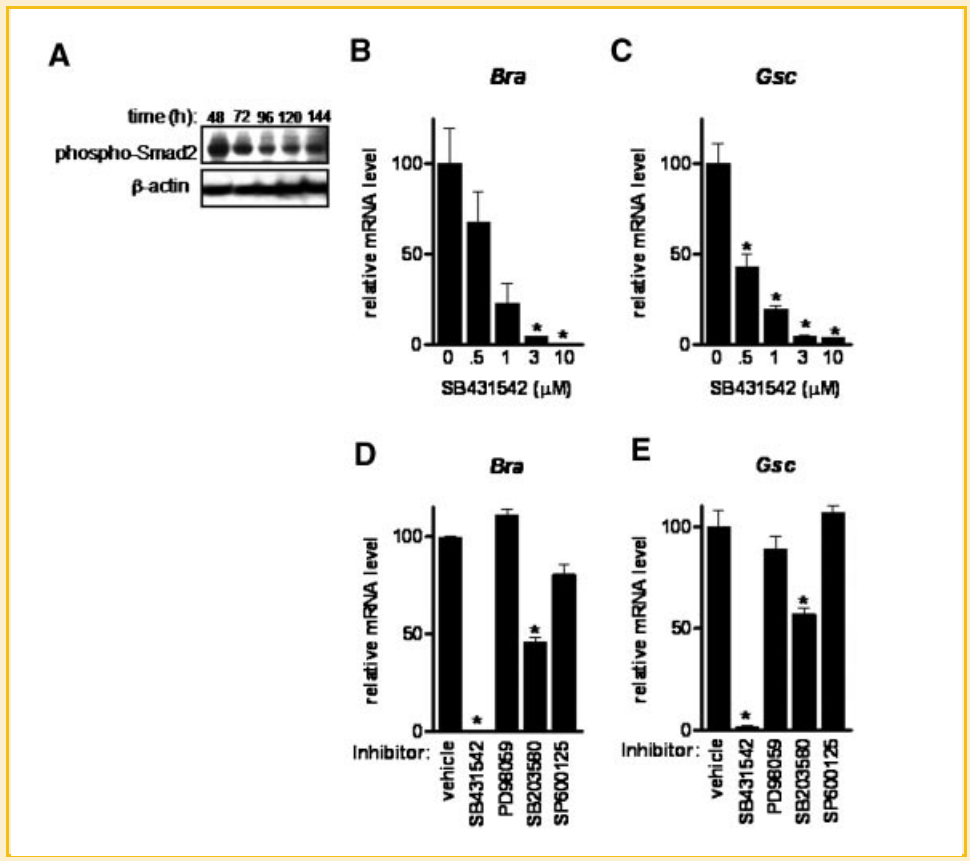

Fig. 3. Expression of *Bra* and *Gsc* is related to attenuation of Tgf-β family signaling. A: 3×10^4 cells were plated into tissue culture grade 35-mm dishes. At the indicated times, attached cells were recovered. Phosphorylation at the C-terminal serines of Smad2 was examined by Western blot analysis using equal amounts of proteins in cell lysates. As a loading control, Western blot analysis using anti-β-actin was also carried out. B–E: 8×10^3 cells were plated into tissue culture grade 24-well dishes in the presence of vehicle (0.1% DMSO), the indicated concentration of SB431542 (B,C), SB431542 (10 μM) or inhibitor for the MAP kinase pathway (PD98059 (50 μM), SB203580 (10 μM) and SP600125 (20 μM) (D,E). At 72 h of culture, attached cells were recovered, and quantitative real-time RT-PCR was performed to measure transcripts of *Bra* (B,D) and *Gsc* (C,E). Gene expression was normalized to the transcript of *G3pdh*, and the value in cells treated with vehicle was set to 100. $^*P < 0.05$ as compared with the value in cells treated with vehicle.

unstimulated P19 cells. Indeed, components required for Nodal signaling, that is, *ActRII*, *ActRIIB*, *Alk4*, *Alk7*, *Smad2*, *Smad3* and *Smad4*, were also significantly expressed (Fig. 4).

Signaling of Tgf-βs, Gdf-1, Gdf-8 and Gdf-11 is also mediated via Smad2/3 [Wall et al., 2000; Rotzer et al., 2001; Oh et al., 2002; Cheng et al., 2003; Rebbapragada et al., 2003; Andersson et al., 2006a,b]. In addition, Gdf-1 also functions as a coligand for Nodal [Tanaka et al., 2007]. Thus, it is possible that these ligands may be responsible for *Bra* and *Gsc* induction in unstimulated P19 cells. In fact, significant expression of *Tgf-β2* and *Gdf-1* and slight expression of *Gdf-11* were detected, and signaling components for these ligands were also expressed at the mRNA level: *TβRII* as a type II receptor and *Alk5* as a type I receptor for Tgf-β2 [Rotzer et al., 2001], *ActRIIB* and *Alk4/7* for Gdf-1 [Wall et al., 2000; Cheng et al., 2003; Andersson et al., 2006a], and *ActRII/IIB* and *Alk4/5* for Gdf-11 [Oh et al., 2002; Andersson et al., 2006b]. However, in view of higher expression of the ligands at 120 h of the culture compared to 48 h (Fig. 4), Tgf-β2, Gdf-1 and Gdf-11 are unlikely to be responsible for changes in the expression of *Bra* and *Gsc* in unstimulated P19 cells, because *Bra* and *Gsc* are down-regulated at 120 h of culture.

Quantitative real-time RT-PCR analyses revealed that expression of *Nodal* and *Cripto* were the highest at 48 h of culture, and that these levels were decreased to below 20% at 72 h of the culture (Fig. 5A). In contrast, consistent with the results of RT-PCR analyses (Fig. 4), expression of *Gdf-1* was significantly increased with time of culture and *Gdf-11* expression also tended to increase with time, except for at 72 h of culture. These results suggest that down-regulation of *Nodal* and *Cripto* with time of culture is not a non-specific event. Expression of *Nodal* and *Cripto* during the earlier phase of the culture indicated a rapid up-regulation of both genes, which resembled to time-course changes in *Gsc* but not *Bra* (Figs. 1C and 5B).

Furthermore, the level of *Nodal* and *Cripto* was decreased with increasing SB431542 (Fig. 5C,D), and the effects of SB431542 on these genes were comparable with those on *Bra* and *Gsc* (Fig. 3B,C). Notably, the IC_{50} concentrations of *Nodal*, *Cripto*, *Bra* and *Gsc* were 0.59, 0.42, 0.71, and 0.42 μM, respectively. Consistent with time-related changes in gene expression, the effects of SB431542 on *Nodal*/*Cripto* and *Gdf-1*/*-11* differed. However, the down-regulation of *Gdf-1* in response to SB431542 treatment was less evident

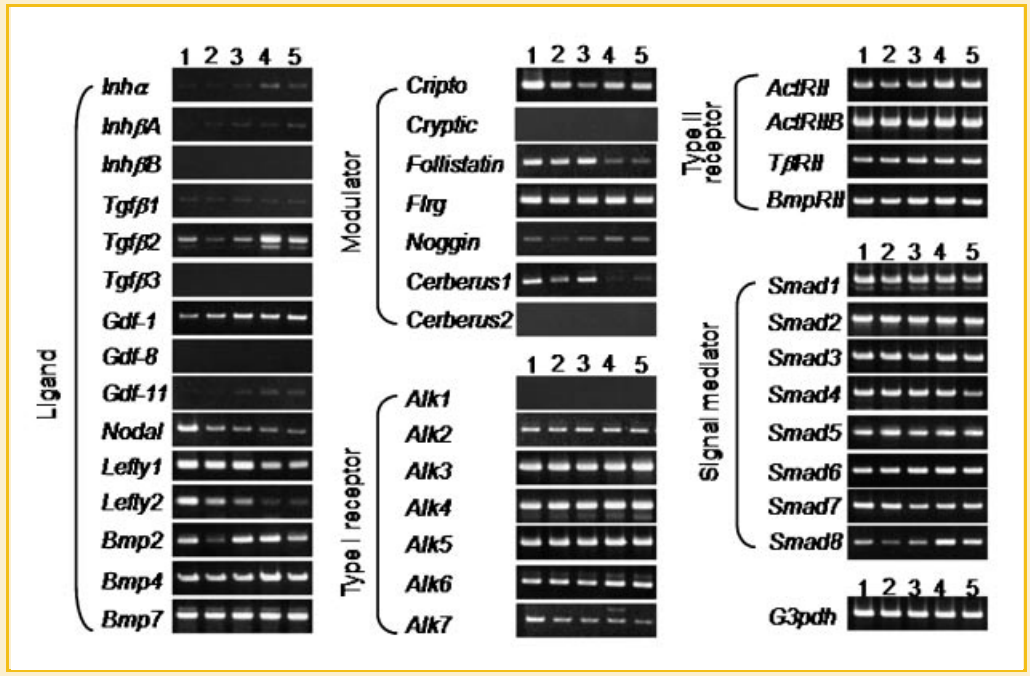

Fig. 4. Expression of molecules related to signaling of the Tgf-β family. 8×10^3 cells were plated into tissue culture grade 24-well dishes. Culture time-related expression of the indicated molecules was examined by RT-PCR. Lanes 1–5 indicate expression at 48, 72, 96, 120, and 144 h, respectively.

(Fig. 5E), and the level of *Gdf-11* tended to be increased by treatment with SB431542 (Fig. 5F). Furthermore, expression of neuroectodermal genes (*Mash-1* and *Pax-6*) was also increased with increasing concentrations of SB431542 (Fig. 5G,H).

To examine positive regulation of *Bra* and *Gsc* by Nodal-Cripto, P19 cells were transfected with Nodal-specific dsRNAi for 24 h. Gene knockdown of *Nodal* resulted in a significant decrease in *Nodal* to ~40% (Fig. 6A). The level of *Bra* and *Gsc* also tended to be decreased by *Nodal* knockdown (Fig. 6B and C); the extent of down-regulation of *Bra* was relatively smaller and statistically insignificant, although the decrease was reproducibly detected (data not shown). In contrast, *Pax-6* but not *Mash-1* tended to be increase in P19 cells transfected with *Nodal*-specific dsRNAi, although it was not statistically significant ($P = 0.07$) (Fig. 6D,E). These results indicate that Nodal-Cripto positively regulates mesodermal markers *Bra* and *Gsc* expression, whereas it negatively regulates neuroectodermal markers *Pax-6* in monolayer P19 cells.

CHANGES IN P19 CELLS THEMSELVES, RATHER THAN CHANGES IN CELL POPULATION, CAUSE REGULATORY EXPRESSION OF *Bra* AND *Gsc*

P19 cells are derived from embryonic carcinoma, and are a mixture of cells differing in differentiation stage and lineage [Mummery et al., 1985]. Thus, the changes in expression of *Bra* and *Gsc* in monolayer P19 cells may result from alteration of cell population, (un)differentiation of P19 cells, or both. To distinguish between these possibilities, a total of nine cell clones arising from single cell cultures were isolated from P19 cells, and gene expression was examined by RT-PCR (Fig. 7A). All nine clones expressed significant levels of *Nanog* and *Oct-3/4*, indicating pluripotent differentiation activity. On the basis of the expression pattern of neuroectodermal markers (*Mash-1* and *Pax-6*) and mesodermal markers (*Bra* and *Gsc*), cell clones were categorized into four groups: significant expression of both markers (clone #6), insignificant expression of both markers (clone #9), predominant expression of mesodermal markers (clone #1–3, 5, and 8), and predominant expression of neuroectodermal markers (#4 and 7). Doubling time (13–18 h) did not differ markedly between clones, suggesting comparable cell growth between clones differing in differentiation properties (Fig. 7B).

Clone #3 expressed high levels of mesodermal genes / low levels of neuroectodermal genes, while clone #4 expressed low mesodermal genes/high neuroectodermal genes. Treatment of clones #3 and #4 with SB431542 decreased expression of the mesodermal genes, whereas it increased expression of the neuroectodermal genes except *Pax-6* in clone #4 (Fig. 7C–F). In addition, a mixed culture consisting of clone #3 and clone #4 cultured for 72 h exhibited expression of the mesodermal genes and the neuroectodermal genes parallel to the proportion of cell number of the clones (data not shown). These results suggest that alteration of expression of *Bra* and *Gsc* during monolayer culture and in response to SB431542 treatment reflects modulation of P19 cells themselves, rather than changes in cell population. Expression of *Nodal* and *Cripto* was also higher in clone #3, which expressed mesodermal genes strongly, than in clone #4, which expressed mesodermal genes weakly (Fig. 7G,H). In addition, the expression was down-regulated by treatment with SB431542. A strong relationship between *Bra/Gsc* expression and *Nodal/Cripto* expression in P19 cell clones also

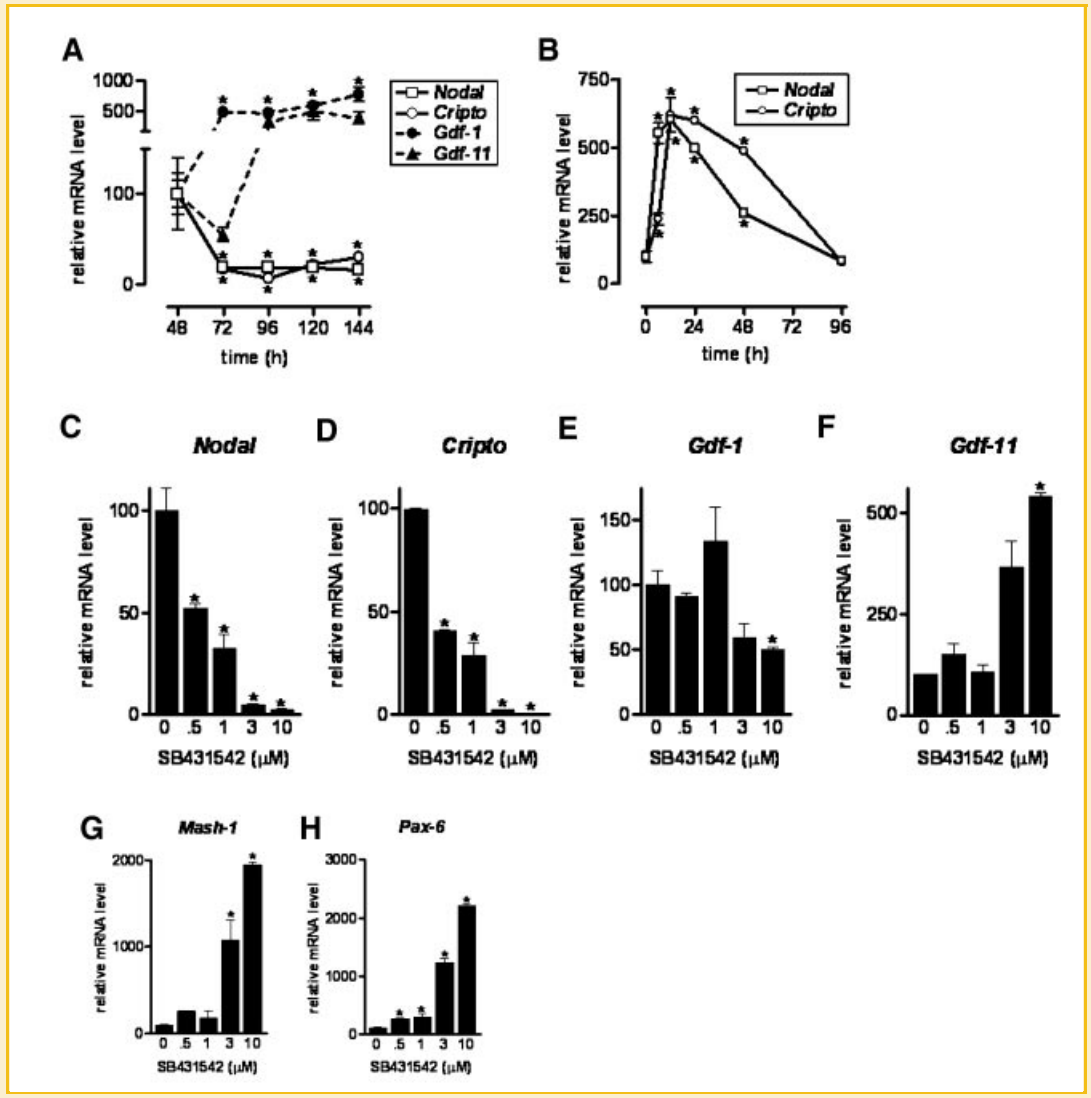

Fig. 5. Expression of *Nodal* and *Cripto* but not *Gdf-1* and *Gdf-11* is decreased with time of culture and by treatment with the ALK4/5/7 inhibitor SB431542 in P19 cells. A,B: 8×10^3 cells were plated into tissue culture grade 24-well dishes. At the indicated times, attached cells were recovered. C–H: 8×10^3 cells were plated into tissue culture grade 24-well dishes in the presence of vehicle (0.1% DMSO) or the indicated concentration of SB431542, an inhibitor for Alk4/5/7. At 72 h of culture, attached cells were recovered. Quantitative real-time RT-PCR was performed to measure transcripts of *Nodal* (A–C), *Cripto* (A,B,D), *Gdf-1* (A,E), *Gdf-11* (A,F), *Mash-1* (G) and *Pax-6* (H). Gene expression was normalized to the transcript level of *G3pdh*, and the value at 48 h (A) or 0 h (B) of culture or that of cells treated with vehicle (C–H) was set to 100. $^*P < 0.05$ as compared with the value at 48 h (A) or 0 h (B) or that cells treated with vehicle (C–H).

suggest expression of *Bra* and *Gsc* regulated by the Nodal-Cripto pathway.

To verify direct regulation of *Bra* and *Gsc* expression by the Nodal pathway, we further examined effects of exogenous administration of Nodal (Fig. 8). Although exogenous Nodal did not significantly affect the levels of *Bra* and *Gsc* in clone #3 (Fig. 8A,B), it up-regulated *Bra* and *Gsc* in a dose dependent manner in clone #4 (Fig. 8C,D).

MONOLAYER P19 CELLS SECRETE INHIBITORY MOLECULES FOR *NODAL* EXPRESSION

Next, to explore the regulation of *Nodal* and *Cripto* expression in monolayer P19 cells, the involvement of two factors was examined: FCS in culture medium and molecule(s) produced during P19 cell culture. To examine the effect of FCS, 40% and 80% of the medium (αMEM with 6% FCS) was replaced with αMEM lacking FCS (40% MEM, i.e., 3.6% FCS, and 80% MEM, i.e., 1.2% FCS, respectively). In addition, to examine the effects of secreted molecule(s) during monolayer culture of P19 cells, 40% and 80% of the medium was replaced with the conditioned medium (CM) which is the culture supernatant of P19 cells maintained with αMEM containing 6% FCS for 144 h (40% CM containing 3.6% fresh FCS and 80% CM containing 1.2% fresh FCS, respectively) (Fig. 9A).

Decreasing the FCS concentration significantly decreased transcripts of *Nodal* and *Cripto* in a dose-dependent manner, suggesting that serum has the ability to increase expression of *Nodal*

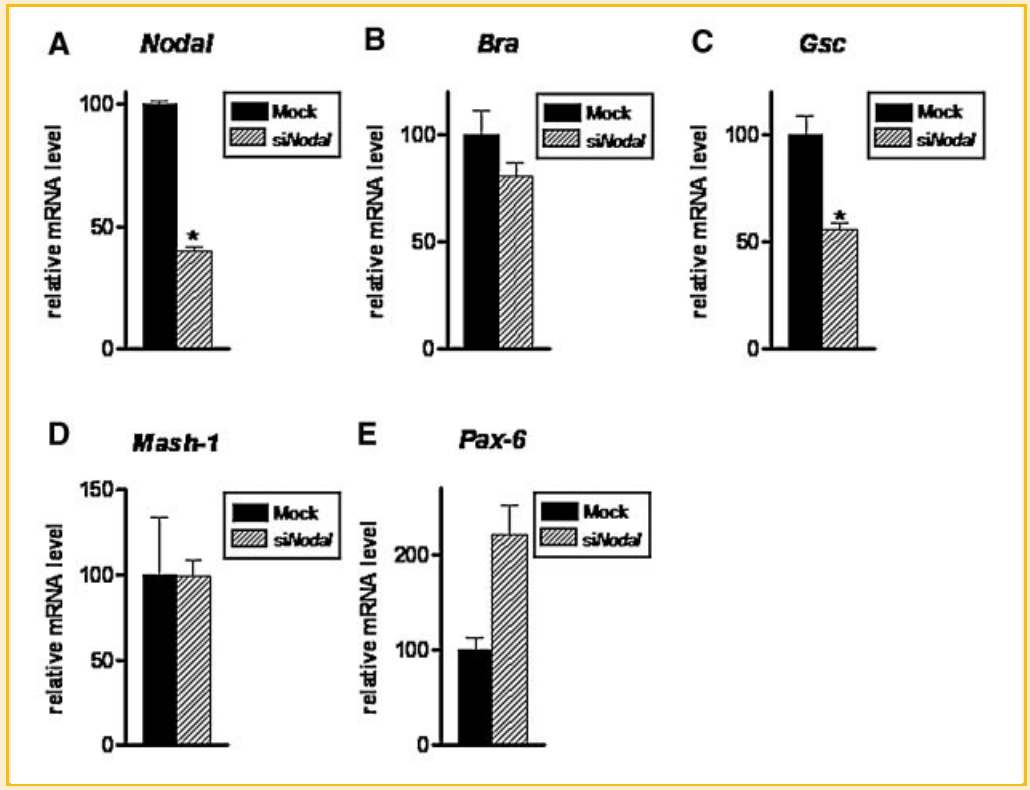

Fig. 6. Knockdown of *Nodal* induces decrease in *Bra* and *Gsc* and increase in *Mash-1* and *Pax-6*. 5×10^4 cells were plated into tissue culture grade 24-well dishes, and treated with or without *Nodal*-specific dsRNAi. At 48 h of culture, cells were recovered, and quantitative real-time RT-PCR was performed to measure transcripts of *Nodal* (A), *Bra* (B), *Gsc* (C), *Mash-1* (D), and *Pax-6* (E). Gene expression was normalized to the transcript level of *G3pdh*, and the expression in mock-treated cells was set to 100. $^*P < 0.05$ as compared with the value in mock-treated cells.

and *Cripto* (Fig. 9B,C). As compared to the control treatment, addition of the culture supernatant of P19 cells resulted in lower expression of *Nodal* and *Cripto* ($P < 0.05$), which was also dose-dependent. It is possible that factor(s) in FCS contributing to the induction of *Nodal* and *Cripto* are depleted during cell culture. However, the lower expression of *Nodal* and *Cripto* caused by addition of CM is not solely explained by the disappearance of stimulatory factors in FCS, because expression of *Nodal* and *Cripto* under 40% CM and 80% CM treatments was lower than that under 40% MEM and 80% MEM treatments, respectively ($P < 0.05$). The further reduction of *Nodal* and *Cripto* by addition of the culture supernatant suggests that molecules inhibiting gene expression are secreted and accumulated during P19 cell culture. Similar effects of FCS and the culture supernatant were observed on expression levels of *Bra* and *Gsc* (Fig. 9D,E). The down-regulation of genes in CM-treated P19 cells was specific event. Expression of *Pax-6* and *Gdf-11* were comparable between the MEM treatments and the corresponding CM treatments, and *Gdf-1* expression was higher in the CM treatment (data not shown).

As a negative regulator of Nodal signaling, Lefty-1/-2, two members of the Tgf-β family are known [Hamada et al., 2002]. To examine whether Lefty is involved in Nodal-mediated regulation of expression of *Bra* and *Gsc* in monolayer P19 cells, Lefty content in the culture supernatant was examined by Western blotting. When the culture supernatant was directly applied to the membrane, immunoreactive Lefty molecules could not be detected (data not shown). A preliminary experiment showed that immunoreactive Lefty was recovered from the resin-binding fraction by Blue Sepharose column chromatography (data not shown). The amount of immunoreactive Lefty in Blue Sepharose resin treated with the culture supernatant was constant during P19 cell culture, whereas a significant amount of Lefty molecules could not be detected in the unbound fraction of the culture supernatant (Fig. 10). These results suggest that unidentified molecules other than Lefty are involved in inhibition of the Nodal pathway during monolayer P19 cell culture, leading to down-regulation of *Nodal* and subsequently *Bra* and *Gsc*.

DISCUSSION

The present study indicated regulatory expression of the mesoderm genes *Bra* and *Gsc* in monolayer murine P19 cells. This expression was seen even in undifferentiated P19 cells, and was positively regulated by the Nodal-Cripto pathway but not the Activin pathway. Considering that Activin induced expression of *Bra* and *Gsc* in *Xenopus* embryos in previous studies [Cho et al., 1991; Latinkic et al., 1997; Dyson and Gurdon, 1998], mesodermal differentiation is regulated by a cell type- or species-specific manner. Expression of

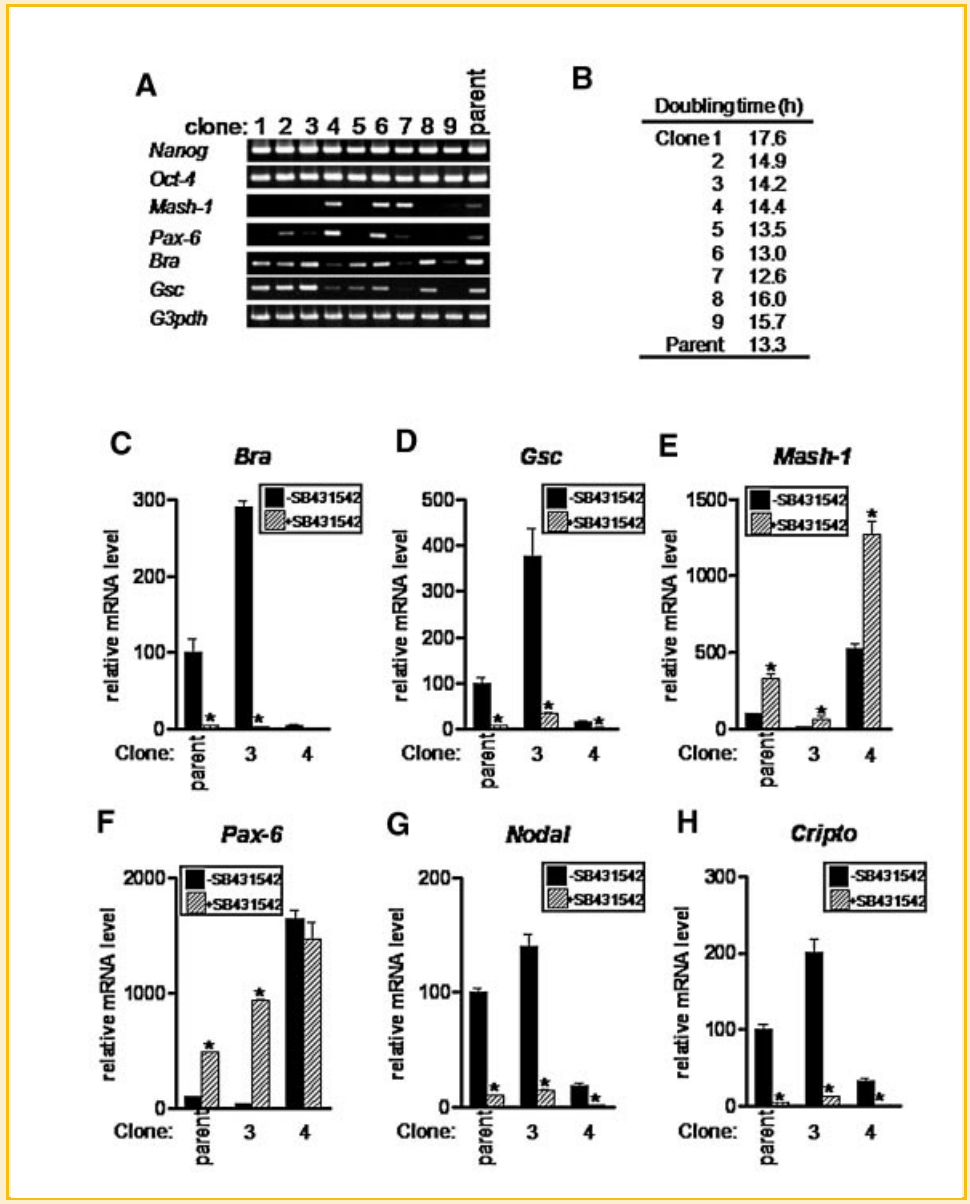

Fig. 7. Changes in expression of *Bra* and *Gsc* result from cell differentiation but not from alteration of cell population in P19 cells. A total of nine clones were isolated from P19 cells. Gene expression of pluripotent differentiation markers (*Nanog* and *Oct-3/4*), neuroectodermal markers (*Mash-1* and *Pax-6*), mesodermal markers (*Bra* and *Gsc*), and the housekeeping gene *G3pdh* was examined by RT-PCR (A), and doubling time was determined (B). C–H: 8×10^3 cells of parent P19 cells and clones #3 and #4 were plated into tissue culture grade 24-well dishes in the presence of vehicle (0.1% DMSO) or 1 μM of SB431542, an inhibitor of Alk4/5/7. At 72 h of culture, attached cells were recovered. Quantitative real-time RT-PCR was performed to measure transcripts of *Bra* (C), *Gsc* (D), *Mash-1* (E), *Pax-6* (F), *Nodal* (G) and *Cripto* (H). Gene expression was normalized to the transcript level of *G3pdh*, and the value of parent P19 cells treated with vehicle was set to 100. $^*P < 0.05$ as compared with the value in cells treated with vehicle (C–H).

Nodal is positively regulated by Nodal itself through complex formation of FoxH3-Smad during left lateral plate mesoderm formation in mice [Osada et al., 2000; Saijoh et al., 2000]. Autoregulation of Nodal would also occur in monolayer P19 cells; *Nodal* expression was down-regulated by SB431542, which blocks Smad2/3 phosphorylation-induced complex formation with FoxH through inhibiting Alk4/5/7 kinase activity. The monolayer P19 cells secreted unidentified molecules inhibiting Nodal autoregulation, which caused dynamic changes in *Bra* and *Gsc* expression.

The present results that unidentified P19 cells significantly expressed *Bra* and *Gsc* contradict from previous results [Pruitt, 1994; Pratt et al., 1998]. The reason of the inconsistent results is unclear. P19 cells used in this study expressed the pluripotent differentiation markers, and actually differentiated into neuron-like cells by aggregation and RA treatment. Considering that P19 cells are a mixture of cells differing in lineage as shown in Figure 7A, the differences in cell population are likely to cause the discrepant pattern of gene expression; major population of P19 cells may be

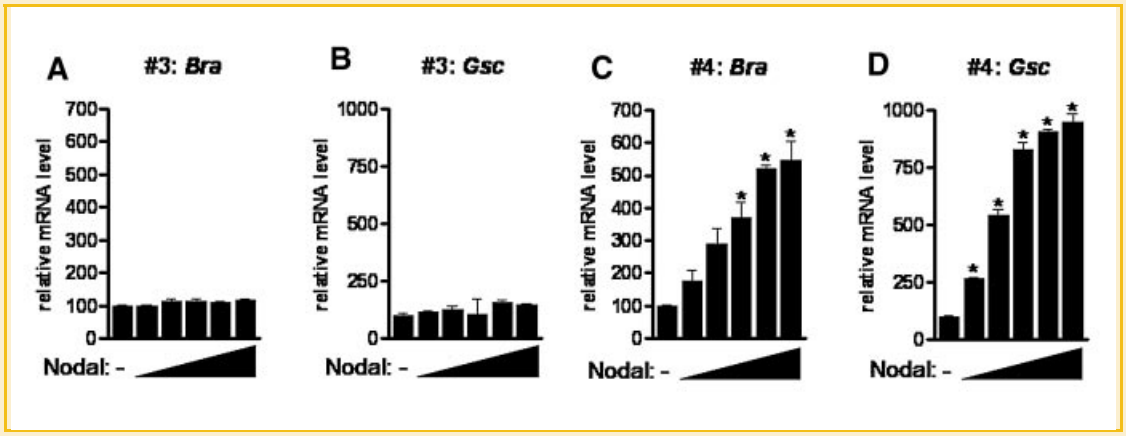

Fig. 8. Exogenous Nodal up-regulates *Bra* and *Gsc* in a P19 cell clone expressing lower *Nodal*, *Bra* and *Gsc*. 1×10^5 cells from clone #3 (A,B) or clone #4 (C,D) were plated into tissue culture grade 24-well dishes, and treated with recombinant mouse Nodal (0, 0.39, 1.6, 6.3, 25, or 100 nM). At 48 h of culture, cells were recovered, and quantitative real-time RT-PCR was performed to measure transcripts of *Bra* (A,C) and *Gsc* (B,D). Gene expression was normalized to the transcript level of *G3pdh*, and the expression in cells treated without exogenous Nodal was set to 100. $^*P < 0.05$ as compared with the value in cells treated without exogenous Nodal.

cells like clone #9 in this study that expressed neither mesodermal genes nor *Nodal* (data not shown). In fact, a positive relationship between mesodermal genes expression and *Nodal* expression was detected in #3 and #4 clones (Fig. 7C,D,G), and Shoji et al. (1998) also observed no significant expression of *Bra* in monolayer P19 cells expressing *Nodal* at the minimal level.

Exogenous Nodal clearly up-regulated both *Bra* and *Gsc* expression in monolayer P19 cells expressing lower *Nodal* (Fig. 8C,D), whereas down-regulation of *Bra* and *Gsc* resulting from knockdown of *Nodal* was limited; especially decrease in *Bra* expression was not statistically significant in each experiment. The smaller effect resulting from *Nodal* knockdown on *Bra* expression may indicate that the protein depletion achieved was insufficient. Alternatively, factors other than Nodal-Cripto are also involved in *Bra* expression. The results that time-course changes in *Bra* expression were different from those in *Nodal* and *Cripto* expression during the earlier phase of culture support this possibility, that is, *Gsc* expression is directly regulated by the Nodal-Cripto pathway,

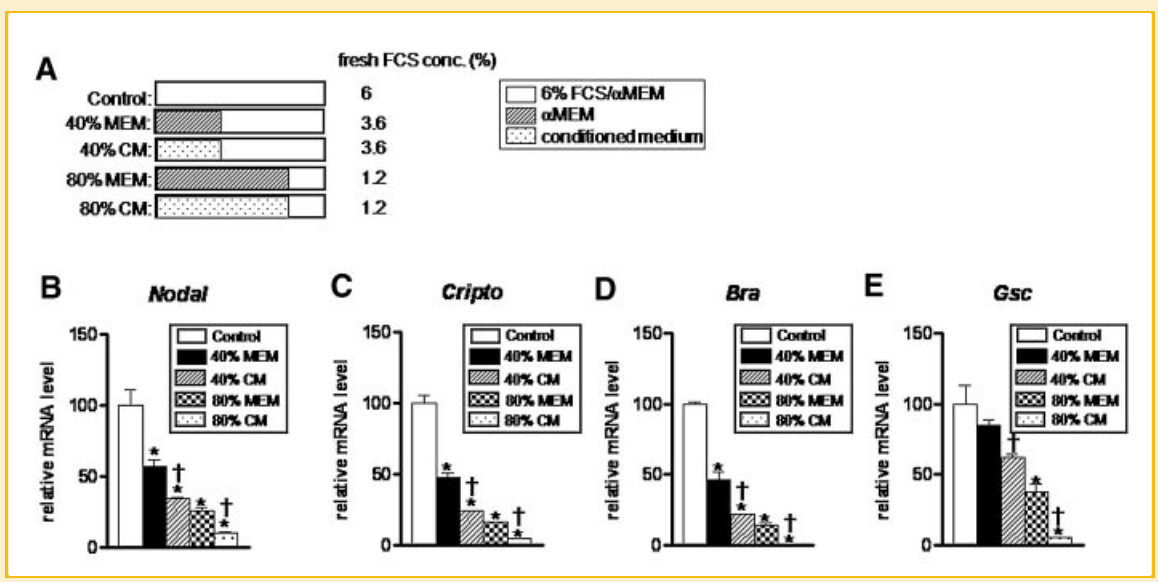

Fig. 9. FCS and molecules secreted into culture medium of P19 cells serve, respectively, as stimulatory and inhibitory factors on the expression of *Nodal*, *Cripto*, *Bra* and *Gsc* in P19 cells. 8×10^3 cells were plated into tissue culture grade 24-well dishes. A: Cells were cultured in αMEM with 6% FCS (control), mixture of αMEM and αMEM with 6% FCS at a ratio of 40:60 (40% MEM) or 80:20 (80% MEM), and mixture of the culture supernatant of P19 cells, which was cultured for 144 h in αMEM with 6% FCS, and αMEM with 6% FCS at a ratio of 40:60 (40% CM) or 80:20 (80% CM). At 72 h of culture, attached cells were recovered. Quantitative real-time RT-PCR was performed to measure transcripts of *Nodal* (B), *Cripto* (C), *Bra* (D), and *Gsc* (E). Gene expression was normalized to the transcript level of *G3pdh*, and the value of the control group, that is, P19 cells cultured in αMEM with 6% FCS was set to 100. * and $^\dagger P < 0.05$ as compared with the value of control and that of MEM group that contains the same concentration of fresh FCS, respectively.

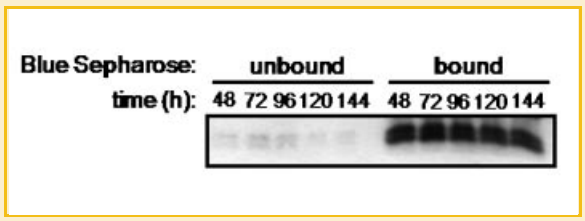

Fig. 10. Lefty content in the culture supernatant is constant during P19 cell culture. 3×10^4 cells were plated into tissue culture grade 35-mm dishes. At the indicated times, the culture supernatant was collected. The culture supernatant was incubated with Blue Sepharose beads, and unbound and bound proteins were subjected to Western blot analysis.

whereas the regulation of *Bra* expression is indirect. The relationship between *Bra* and *Gsc* expression and the Nodal-Cripto pathway in P19 cells may be different from that in in vivo zebrafish embryos. In animal caps of zebrafish, as compared to *Gsc* expression, *Bra* expression is more sensitively regulated by Squint, a zebrafish Nodal [Chen and Schier, 2001]. It is possible that *Bra* expression is significantly regulated by the other pathway in P19 cells. Wnt signals are known to induce *Bra* expression in mouse ES cells [Arnold et al., 2000].

Irrespective of significant expression of mesodermal genes under undifferentiated condition, P19 cells could change morphology and gene expression resembling neurons. Deducing from changes in mesodermal genes expression in P19 clones, it is suggested that the changes did not result from cell population but cell differentiation. There are two possibilities on the transdifferentiation; (1) dedifferentiation of mesodermal cells and subsequent differentiation into ectodermal cells, and (2) direct transdifferentiation of mesodermal cells into ectodermal cells. In view of expression of pluripotent differentiation genes in addition to mesodermal genes in monolayer P19 cells, the latter may be also possible.

The present study indicated that decreasing concentrations of FCS decreased expression of *Bra* and *Gsc* in a dose-dependent manner, suggesting that FCS contains molecules to stimulate these genes. TGF-β, which is present in FCS, shares the same signaling pathway as Nodal and Activin as described above [Derynck and Zhang, 2003; Massagué et al., 2005]. However, P19 cells are not responsive to TGF-β; neither Smad2 phosphorylation nor induction of TGF-β-responsive genes were detected in response to TGF-β treatment (data not shown). Thus, it is unlikely that decreased TGF-β in FCS is responsible for down-regulation of *Bra* and *Gsc* expression in P19 cells cultured with lower FCS concentrations.

SB431542 inhibited expression of *Bra* and *Gsc*, whereas it stimulated expression of *Mash-1* and *Pax-6*. The effect was also detected in a P19 cell clone expressing significant levels of *Bra* and *Gsc*. Although treatment with SB431542 did not result in morphological changes resembling nerve cells in monolayer P19 cells, the findings suggest the direct differentiation of mesodermal cells toward neuroectodermal cells in P19 cells. A recent study revealed that disruption of Nodal signaling led to appearance of neurons in mouse embryos [Camus et al., 2006]. Since differentiation into neurons is the default pathway in *Xenopus* [Muñoz-Sanjuán and Brivanlou, 2002], control of the Nodal pathway may also be important in differentiation/de-differentiation of P19 cells. Thus, further studies are needed to identify molecules regulating *Nodal* and *Cripto* expression in monolayer P19 cells, which may lead to a better understanding of the molecular bases of mesodermal formation as well as neurogenesis.

ACKNOWLEDGMENTS

This work was supported by Grant-in-Aid for Scientific Research (17580262 to M.M. and 15580268 and 18580299 to M.F.) from Japan Society for the Promotion of Science and grants for Graduate Schools from The Foundation for Japanese Private School Promotion (to K.N., M.M. and M.F.).

REFERENCES

Andersson O, Reissmann E, Jornvall H, Ibanez CF. 2006a. Synergistic interaction between Gdf1 and Nodal during anterior axis development. Dev Biol 293:370–381.

Andersson O, Reissmann E, Ibanez CF. 2006b. Growth differentiation factor 11 signals through the transforming growth factor-β receptor ALK5 to regionalize the anterior-posterior axis. EMBO Rep 7:831–837.

Arnold SJ, Stappert J, Bauer A, Kispert A, Herrmann BG, Kemler R. 2000. Brachyury is a target gene of the Wnt/beta-catenin signaling pathway. Mech Dev 91:249–258.

Bensadoun A, Weinstein D. 1976. Assay of proteins in the presence of interfering materials. Anal Biochem 70:241–250.

Blum M, Gaunt SJ, Cho KW, Steinbeisser H, Blumberg B, Bittner D, De Robertis EM. 1992. Gastrulation in the mouse: The role of the homeobox gene goosecoid. Cell 69:1097–1106.

Boncinelli E, Mallamaci A. 1995. Homeobox genes in vertebrate gastrulation. Curr Opin Genet Dev 5:619–627.

Boudjelal M, Taneja R, Matsubara S, Bouillet P, Dolle P, Chambon P. 1997. Overexpression of Stra13, a novel retinoic acid-inducible gene of the basic helix-loop-helix family, inhibits mesodermal and promotes neuronal differentiation of P19 cells. Genes Dev 11:2052–2065.

Burdon T, Smith A, Savatier P. 2002. Signalling, cell cycle and pluripotency in embryonic stem cells. Trends Cell Biol 12:432–438.

Callahan JF, Burgess JL, Fornwald JA, Gaster LM, Harling JD, Harrington FP, Heer J, Kwon C, Lehr R, Mathur A, Olson BA, Weinstock J, Laping NJ. 2002. Identification of novel inhibitors of the transforming growth factor β1 (TGF-β1) type 1 receptor (ALK5). J Med Chem 45:999–1001.

Camus A, Perea-Gomez A, Moreau A, Collignon J. 2006. Absence of Nodal signaling promotes precocious neural differentiation in the mouse embryo. Dev Biol 295:743–755.

Chambers I, Colby D, Robertson M, Nichols J, Lee S, Tweedie S, Smith A. 2003. Functional expression cloning of Nanog, a pluripotency sustaining factor in embryonic stem cells. Cell 113:643–655.

Chen Y, Schier AF. 2001. The zebrafish Nodal signal Squint functions as a morphogen. Nature 411:607–610.

Cheng SK, Olale F, Bennett JT, Brivanlou AH, Schier AF. 2003. EGF-CFC proteins are essential coreceptors for the TGF-β signals Vg1 and GDF1. Genes Dev 17:31–36.

Cho KW, Blumberg B, Steinbeisser H, De Robertis EM. 1991. Molecular nature of Spemann's organizer: The role of the Xenopus homeobox gene goosecoid. Cell 67:1111–1120.

Derynck R, Zhang YE. 2003. Smad-dependent and Smad-independent pathways in TGF-β family signalling. Nature 425:577–584.

Dyson S, Gurdon JB. 1998. The interpretation of position in a morphogen gradient as revealed by occupancy of activin receptors. Cell 93:557–568.

Funaba M, Ikeda T, Murakami M, Ogawa K, Tsuchida K, Sugino H, Abe M. 2003. Transcriptional activation of mouse mast cell protease-7 by activin and transforming growth factor-β is inhibited by microphthalmia-associated transcription factor. J Biol Chem 278:52032–52041.

Hamada H, Meno C, Watanabe D, Saijoh Y. 2002. Establishment of vertebrate left-right asymmetry. Nat Rev Genet 3:103–113.

Inman GJ, Nicolas FJ, Callahan JF, Harling JD, Gaster LM, Reith AD, Laping NJ, Hill CS. 2002. SB-431542 is a potent and specific inhibitor of transforming growth factor-β superfamily type I activin receptor-like kinase (ALK) receptors ALK4, ALK5, and ALK7. Mol Pharmacol 62:65–74.

Johnson JE, Birren SJ, Anderson DJ. 1990. Two rat homologues of Drosophila achaete-scute specifically expressed in neuronal precursors. Nature 346: 858–861.

Johnson JE, Zimmerman K, Saito T, Anderson DJ. 1992. Induction and repression of mammalian achaete-scute homologue (MASH) gene expression during neuronal differentiation of P19 embryonal carcinoma cells. Development 114:75–87.

Jones CM, Armes N, Smith JC. 1996. Signalling by TGF-β family members: Short-range effects of Xnr-2 and BMP-4 contrast with the long-range effects of activin. Curr Biol 6:1468–1475.

Jones-Villeneuve EM, McBurney MW, Rogers KA, Kalnins VI. 1982. Retinoic acid induces embryonal carcinoma cells to differentiate into neurons and glial cells. J Cell Biol 94:253–262.

Latinkic BV, Umbhauer M, Neal KA, Lerchner W, Smith JC, Cunliffe V. 1997. The Xenopus Brachyury promoter is activated by FGF and low concentrations of activin and suppressed by high concentrations of activin and by paired-type homeodomain proteins. Genes Dev 11:3265–3276.

Massagué J, Seoane J, Wotton D. 2005. Smad transcription factors. Genes Dev 19:2783–2810.

McBurney MW. 1993. P19 embryonal carcinoma cells. Int J Dev Biol 37:135–140.

McBurney MW, Jones-Villeneuve EM, Edwards MK, Anderson PJ. 1982. Control of muscle and neuronal differentiation in a cultured embryonal carcinoma cell line. Nature 299:165–167.

Meno C, Saijoh Y, Fujii H, Ikeda M, Yokoyama T, Yokoyama M, Toyoda Y, Hamada H. 1996. Left-right asymmetric expression of the TGF β-family member lefty in mouse embryos. Nature 381:151–155.

Mitsui K, Tokuzawa Y, Itoh H, Segawa K, Murakami M, Takahashi K, Maruyama M, Maeda M, Yamanaka S. 2003. The homeoprotein Nanog is required for maintenance of pluripotency in mouse epiblast and ES cells. Cell 113:631–642.

Mummery CL, Feijen A, van der Saag PT, van den Brink CE, de Laat SW. 1985. Clonal variants of differentiated P19 embryonal carcinoma cells exhibit epidermal growth factor receptor kinase activity. Dev Biol 109:402–410.

Muñoz-Sanjuán I, Brivanlou AH. 2002. Neural induction, the default model and embryonic stem cells. Nat Rev Neurosci 3:271–280.

Niwa H. 2001. Molecular mechanism to maintain stem cell renewal of ES cells. Cell Struct Funct 26:137–148.

O'Shea KS. 2004. Self-renewal vs. differentiation of mouse embryonic stem cells. Biol Reprod 71:1755–1765.

Oh SP, Yeo CY, Lee Y, Schrewe H, Whitman M, Li E. 2002. Activin type IIA and IIB receptors mediate Gdf11 signaling in axial vertebral patterning. Genes Dev 16:2749–2754.

Okamoto K, Okazawa H, Okuda A, Sakai M, Muramatsu M, Hamada H. 1990. A novel octamer binding transcription factor is differentially expressed in mouse embryonic cells. Cell 60:461–472.

Osada SI, Saijoh Y, Frisch A, Yeo CY, Adachi H, Watanabe M, Whitman M, Hamada H, Wright CV. 2000. Activin/nodal responsiveness and asymmetric expression of a Xenopus nodal-related gene converge on a FAST-regulated module in intron 1. Development 127:2503–2514.

Pachernik J, Bryja V, Esner M, Kubala L, Dvorak P, Hampl A. 2005. Neural differentiation of pluripotent mouse embryonal carcinoma cells by retinoic acid: Inhibitory effect of serum. Physiol Res 54:115–122.

Pratt MA, Crippen C, Hubbard K, Menard M. 1998. Deregulated expression of the retinoid X receptor alpha prevents muscle differentiation in P19 embryonal carcinoma cells. Cell Growth Differ 9:713–722.

Pruitt SC. 1994. Primitive streak mesoderm-like cell lines expressing Pax-3 and Hox gene autoinducing activities. Development 120:37–47.

Rashbass P, Cooke LA, Herrmann BG, Beddington RS. 1991. A cell autonomous function of Brachyury in T/T embryonic stem cell chimaeras. Nature 353:348–351.

Rebbapragada A, Benchabane H, Wrana JL, Celeste AJ, Attisano L. 2003. Myostatin signals through a transforming growth factor β-like signaling pathway to block adipogenesis. Mol Cell Biol 23:7230–7242.

Rotzer D, Roth M, Lutz M, Lindemann D, Sebald W, Knaus P. 2001. Type III TGF-β receptor-independent signalling of TGF-β2 via TβRII-B, an alternatively spliced TGF-β type II receptor. EMBO J 20:480–490.

Saijoh Y, Adachi H, Sakuma R, Yeo CY, Yashiro K, Watanabe M, Hashiguchi H, Mochida K, Ohishi S, Kawabata M, Miyazono K, Whitman M, Hamada H. 2000. Left-right asymmetric expression of lefty2 and nodal is induced by a signaling pathway that includes the transcription factor FAST2. Mol Cell 5:35–47.

Shoji H, Nakamura T, van den Eijnden-van Raaij AJ, Sugino H. 1998. Identification of a novel type II activin receptor, type IIA-N, induced during the neural differentiation of murine P19 embryonal carcinoma cells. Biochem Biophys Res Commun 246:320–324.

Smith JC, Price BM, Van Nimmen K, Huylebroeck D. 1990. Identification of a potent Xenopus mesoderm-inducing factor as a homologue of activin A. Nature 345:729–731.

Tanaka C, Sakuma R, Nakamura T, Hamada H, Saijoh Y. 2007. Long-range action of Nodal requires interaction with GDF1. Genes Dev 21:3272–3282.

Technau U. 2001. Brachyury, the blastopore and the evolution of the mesoderm. Bioessays 23:788–794.

Wall NA, Craig EJ, Labosky PA, Kessler DS. 2000. Mesendoderm induction and reversal of left-right pattern by mouse Gdf1, a Vg1-related gene. Dev Biol 227:495–509.

Walther C, Gruss P. 1991. Pax-6, a murine paired box gene, is expressed in the developing CNS. Development 113:1435–1449.

Whitman M. 2001. Nodal signaling in early vertebrate embryos: Themes and variations. Dev Cell 1:605–617.